TECHNICAL MEMORANDUM

X-419

CAVITATION PERFORMANCE OF AN 83° HELICAL INDUCER OPERATED IN LIQUID HYDROGEN

By George W. Lewis, Jr., Edward R. Tysl,
and Donald M. Sandercock

Lewis Research Center
Cleveland, Ohio

NATIONAL AERONAUTICS AND SPACE ADMINISTRATION

WASHINGTON

March 1961

NATIONAL AERONAUTICS AND SPACE ADMINISTRATION

TECHNICAL MEMORANDUM X-419

CAVITATION PERFORMANCE OF AN 83° HELICAL INDUCER OPERATED IN LIQUID HYDROGEN*

By George W. Lewis, Jr., Edward R. Tysl, and Donald M. Sandercock

SUMMARY

A flat-plate helical inducer with a constant tip diameter of 1.88 inches was built and tested in liquid hydrogen. The inducer, which was made of 2024-T4 aluminum, had two constant-thickness blades and a constant 0.4 hub-tip radius ratio.

The noncavitating performance was similar to that observed for flat-plate inducers operated in water. A slight inflection point was noted in the characteristic line at about the mean flow range. This is compared with similar observations obtained from axial-flow-pump performance in water.

Cavitation performance is discussed in terms of cavitation number. As inlet pressure was reduced, flow conditions resulting in cavitation number values of zero were obtained in which the performance did not indicate cavitation breakdown. These observations are compared with results obtained from similar inducers operating in water. Further decreases of inlet pressure produced a series of apparently stable operating points, as well as could be ascertained from the instrumentation involved. Two flow models indicating basic types of flow that could exist under these conditions are advanced, and the state of the flow at the inducer inlet is considered to be an application of these flow models to different degrees. While the data obtained apparently substantiated the existence of one of the models, it could not be ascertained to what degree the model applied in this investigation. The need is indicated for a careful location of pump inlet instrumentation and an additional parameter to describe flow conditions adequately under these operating conditions.

Radial distributions of head rise are presented for several values of flow under both cavitating and noncavitating conditions. A section

*Title, Unclassified.

describing the operational and mechanical experiences encountered in this investigation is also included.

INTRODUCTION

Component research and development have become increasingly important for both chemical (liquid) propellant and nuclear rocket systems. In both applications, weight reduction of individual components is of prime importance. Consideration of low weight and high thrust in chemical-propelled rocket engines results in low propellant tank pressures and high combustion-chamber pressures. The component which satisfies these two extremes of pressure is the turbopump unit. Its function is to take the low-pressure propellant from the storage tank and deliver it at a high pressure to the combustion chamber. Weight of the turbopump varies inversely as rotational speed (i.e., as speed increases, required diameter of pump and drive turbine decreases). Therefore, increasing rotational speed would lower both pump and drive turbine weights.

As speed increases, deterioration of pump performance generally takes place because of cavitation before mechanical or stress limitations are reached. Cavitation can be described as a flow condition within the pump at which local pressure reaches or drops below the vapor pressure of the fluid, causing vapor bubbles to form. As the vapor bubbles reach regions of higher pressure, they collapse and may cause structural damage to the pump as well as deterioration of pump performance. A conventional parameter for determining effect of cavitation on performance for geometrically similar pumps is suction specific speed. This parameter indicates that the ability of a given pump to operate at increased suction specific speeds could be reflected as an increase in speed, and/or a decrease in required propellant tank pressure. Several methods of obtaining higher suction specific speeds have been suggested (ref. 1); the one investigated herein is the cavitating inducer.

The cavitating inducer is usually an axial inlet stage with low head rise and high flow characteristics and is designed to operate with cavitation. It adds energy so that any vapor formed is recondensed, generally without structural damage. Thus, the succeeding high-pressure pump stages can operate in essentially a noncavitating environment.

Considerable experimental work on cavitating inducers, generally operating in water, has been reported. However, it is well known that the net positive suction head requirements for a given drop in performance of a pump differ with each fluid. Some attempt to correlate these different requirements based on the physical properties of various fluids has been made (refs. 2 and 3). The growing interest in the use of liquid hydrogen as a propellant, both in chemical and nuclear rockets, indicates a need for information on suction performance of inducers operating in this fluid for both design purposes and correlation with available experimental work.

To observe the performance of an inducer operating in liquid hydrogen, a 1.88-inch-diameter 83° flat-plate helical inducer was designed and tested at the Lewis Research Center over a range of operating conditions. The aluminum inducer was designed with two constant-thickness blades and a constant hub-tip radius ratio of 0.4.

This report presents the measured cavitating and noncavitating performance of the inducer and a summary of operational problems encountered in testing with liquid hydrogen. The inducer performance is compared with helical inducers operated in water.

SYMBOLS

g acceleration due to gravity, 32.17 ft/sec^2

H total head, ft

ΔH pump total head rise, ft

H_{sv} net positive suction head, $H_1 - h_{v,1}$, ft

h static head, ft

h_v vapor head, ft

k cavitation number or index $= \frac{h_1 - h_{v,1}}{V_{1,t}'^2/2g} = \frac{2g(H_{sv})}{U_t^2(1 + \varphi^2)} - \frac{\varphi^2}{1 + \varphi^2}$

N pump rotational speed, rpm

Q flow, gal/min

S suction specific speed, $\frac{N\sqrt{Q}}{H_{sv}^{0.75}}$

T temperature, °R

U blade speed, ft/sec

V fluid velocity, ft/sec

φ dimensionless flow coefficient, $V_{a,1}/U_{t,1}$

ψ dimensionless head coefficient, $g\frac{\Delta H}{U_{t,1}^2}$

Subscripts:

a axial

t tip

1 rotor inlet

Superscripts:

' relative to rotor

APPARATUS AND PROCEDURE

Inducer Rotor

The simplest type of inducer form from the standpoint of manufacture (constant lead screw) and one which has shown promising performance characteristics is the flat-plate helical inducer. Helix angles that have received attention fall in an approximate range from 75° to 85°, with the higher angled inducers associated with increased suction-specific-speed application. The particular helicoidal inducer chosen for this investigation incorporated a helix angle of 83°, two constant-thickness (0.060 in.) blades, an outer diameter of 1.88 inches, and a constant hub-tip radius ratio of 0.4. The rotor, which was machined from 2024-T4 aluminum, is shown in figure 1. The size of the rotor was primarily determined by modification limitations on an existing pump test assembly (ref. 4). Clearance between blade tip and the outer casing was approximately 0.010 inch.

Test Facility

A schematic diagram of the liquid-hydrogen inducer pump test loop is presented in figure 2. With the exception of some piping changes due to the addition of a second Dewar and minor modification of the pump package to accommodate the inducer pump rotor, the test facility is the same as described in reference 4. Therefore, only test loop modifications will be discussed in detail herein.

The flow path of the fluid from the 1000-gallon vacuum-jacketed supply Dewar tank included, in succession, the Venturi flowmeter, pump package, flow control valve, and the 6000-gallon receiver Dewar. The contents of the supply Dewar were replenished by means of the separate transfer line between the two Dewars. A tee was placed in the inlet piping in order to fill the liquid-hydrogen tank of the pump package. Piping in the test loop and transfer line consisted of both rigid and flexible

vacuum-jacketed sections with an inside diameter of 1.5 inches. All valves in the test loop were vacuum-jacketed and remote-controlled. Admission to the hydrogen-gas disposal vent system was made through remote-control valves located on the Dewars and test loop. Other connections necessary to utilize auxiliary systems such as a helium-gas supply, a vacuum connection for purging purposes, and a hydrogen-gas supply for pressurization of the Dewars are indicated in figure 2.

A detailed sketch of the pump package is shown in figure 3. The pump package of reference 4 was modified to allow installation of the inducer rotor, discharge torus, and the bearing and seal housing. The inducer was mounted on the lower end of the pump shaft, which was supported by two bearings. The inducer was separated from the lower bearing by a face seal and a spring-loaded shaft seal. Further bearing and seal information is presented in the appendix. A jack shaft arrangement was utilized to transmit power from the air turbine to the pump shaft. The air turbine of reference 4 was replaced with one having a higher horsepower rating.

Instrumentation

The temperatures were measured using carbon composition resistors. The resistance of this material increases exponentially as temperature decreases in liquid-hydrogen temperature range. All pressures were measured with pressure transducers. Pressure lines from the probes to the transducers were made long to minimize any chance of liquid entering the transducer. A direct measurement of net positive suction head was obtained as described in reference 5. Basically, the system consists of a stagnation pressure tube, a vapor pressure bulb, and a differential pressure measuring device. The most important requirement entering into measurement accuracy is filling the vapor bulb with material which is, as nearly as possible, identical to the fluid being pumped. In this investigation hydrogen gas from the supply Dewar was used. Further details are included in the appendix. Pump speed was measured by means of a magnetic-type pickup and an electronic counter.

Pump inlet. - The pump inlet instrumentation (fig. 3) consisted of three carbon resistor probes circumferentially spaced about the inlet, and a net positive suction head meter located along the longitudinal centerline of the inlet piping. Inlet total pressure was taken from this latter device. The temperature and H_{sv} measuring devices were located approximately 2 inches upstream of the inducer blade leading edge.

Pump discharge. - The inducer discharge measuring station was located approximately 1/4 inch downstream of the blade trailing edge. The instrumentation consisted of two radial rakes each containing two

total-pressure heads. The total-head probes were open-end chamfered tubes spaced at centers of four equal annular areas and set at a calculated mean flow angle.

Flow measuring stations. - Flow was measured by means of a standard ASME Venturi located in a section of the inlet piping. Inlet and Venturi throat pressures were obtained from wall static taps. The carbon resistor for measuring fluid temperature was located just downstream of the Venturi for convenience in mounting and sealing.

Accuracy and reliability. - Because of the limited amount of data (and consequently computations) that could be obtained with this instrumentation, very little can be said concerning the accuracy, or reliability, of the individual measurements. However, some general accuracy values applied to the carbon resistors and pressure transducers used in this investigation are 1 percent of the absolute temperature and 1 percent of full-scale reading, respectively. Applying these values to the measured pressures and temperatures gives the following accuracies:

Temperature	$\pm 0.37^{\circ}$ R
Inlet pressure	± 0.4 lb/sq in. ($\cong \pm 13.2$ ft liq. H_2)
Head rise	± 0.3 lb/sq in. ($\cong \pm 9.9$ ft liq. H_2)
H_{SV}	± 0.4 lb/sq in. ($\cong \pm 13.2$ ft liq. H_2)
	± 0.02 lb/sq in. ($\cong \pm 0.6$ ft liq. H_2)

The net positive suction head was measured with a high-pressure (40 lb/sq in.) transducer during high inlet pressure operation and a low-pressure (2 lb/sq in.) transducer whenever its range was applicable.

Some feel for the reliability of the data may be obtained from table I where the measured inlet temperatures (average of three carbon resistor probes) are compared with a temperature computed from the inlet pressures, H_{SV} pressures, and the vapor pressure curve. With few exceptions the temperatures compare within the accuracy of the carbon resistor probes and show especially close agreement in the area of greatest interest - the low H_{SV} operation. The greater difference at high H_{SV} operation may be due in part to the increased measuring error associated with the high H_{SV} pressure range transducer.

Operating Procedure

The inducer tests were conducted at a constant speed of 35,000 rpm and at various positions of the flow control valve. After the initial purge and cool-down operations during which the pump was rotated at base speed (9000 rpm), desired supply pressure (above cavitation requirements) was set; and pump speed was increased to 35,000 rpm. When the recording potentiometers indicated stable flow conditions, data were recorded on

tape by activating the digital equipment. Data were periodically recorded as inlet pump pressure (H_{SV}) was systematically reduced until the fluid in the supply Dewar was nearly depleted. The pump speed was then reduced to base speed, the flow control valves were closed, and fluid transfer operations begun. When the supply Dewar was refilled, testing was resumed.

The one exception to this procedure occurred for the series of points obtained at an open-throttle position (runs 115 to 131 on table I). For this series the pump was brought up to speed with the supply tank vented to the atmosphere, and then the inlet pressure gradually increased.

During the operation of these tests, numerous operating problems were encountered. Pertinent experiences of this nature are discussed in the appendix.

Calculations

The pressures, temperatures, and speed were all measured on a self-balancing digital potentiometer and recorded on tape. For monitoring purposes and as a back-up to the digital output, speed and certain significant pressures were preserved on strip chart recorders. From accuracy considerations the recording instruments were set up such that positive and small negative differential pressures could be recorded. This resulted in limiting the range of H_{SV} that could be presented.

The necessary equations used herein are self-evident from the definitions of the parameters presented, with the exception of weight flow, which was computed from the standard ASME equation for a Venturi meter. However, some of the considerations and assumptions used in the computations are as follows:

(1) Data taken from a single probe represent a circumferential average of the flow conditions.

(2) The inlet absolute flow velocity has no prewhirl and is constant across the passage. Magnitude of the velocity is computed from measured flow and the geometric area of the inlet passage.

(3) The outlet pressure used to compute overall performance is an arithmetic average of the four total heads on the radial rakes.

(4) Wherever possible, the calculation of cavitation number k was based on H_{SV} measurements. The exceptions to this method occurred when H_{SV} measurements below the lower limit of the recording instrument occurred. For the latter cases the inlet temperature from the carbon

resistor probes was used to obtain fluid vapor pressure as shown in table I.

(5) At the open-throttle position (runs 115 to 131 on table I) the pressure transducer used to measure inlet total pressure was found to be defective. Inlet total pressures for these runs were computed by obtaining a vapor pressure based on inlet temperature (carbon resistors) and adding the observed H_{sv} measurements.

RESULTS AND DISCUSSION

Whenever cavitation tests are conducted, it is convenient to observe the pump performance as a function of some cavitation parameter. The one used herein is the cavitation number, or index, k, which is based upon the upstream static head, vapor head, and the inlet relative dynamic head as defined in the section entitled SYMBOLS.

In addition when evaluating the cavitating performance presented herein or comparing it with similar results, it should be remembered that the data of this investigation were obtained in a fluid whose temperature ranged from 36° to 38° R. The physical properties of liquid hydrogen vary sufficiently with temperature to noticeably affect the cavitation performance.

Noncavitating Performance

The noncavitating overall performance characteristic curve of this 83° helical inducer is shown (as noted) in figure 4 as a plot of head coefficient ψ against flow coefficient φ. The symbols represent actual test points taken at various constant-throttle positions.

The noncavitating characteristic line encompasses all the data points with a k value equal to, or greater than, approximately 0.075. This basis for selecting this value to divide the cavitating and noncavitating performance will be shown more clearly on a later figure. In general, the curve shows the usual inverse relation between head and flow coefficients observed in helical inducers. At a flow coefficient of 0.064 a slight dip in the noncavitating performance curve is noted. A similar inflection point (although slight) has been observed in the results of helical inducers operating in water, while one of a more pronounced nature has been reported in reference 6 for an axial-flow-pump stage operating in water. Reference 6 showed that the dip in the overall performance curve and the initial indication of reverse flow in the hub region of the rotor occur at the same flow coefficient. It was also noted that this small dip region was an unstable operating region insofar as operation at a constant flow coefficient was concerned, and that the maximum

efficiency occurred at a flow coefficient just outside the high flow coefficient end of the dip region.

Figure 5 compares the noncavitating characteristic curve with some results obtained from helical inducers utilizing water as the test fluid (ref. 7 and unpublished NASA data). Although the comparison does not include the results of an inducer with an identical helix angle operated in both fluids, it is evident from figure 5 that the liquid-hydrogen inducer performance fits into the spectrum of inducer performance both in regard to the shape of the characteristic curve and level of performance. This emphasizes the fact, as indicated in other work, that the fluid properties have little effect on the noncavitating head-flow characteristic of a pump. This was also pointed out in reference 2, which reports the results of several pumps tested in liquid hydrogen, liquid nitrogen, and water. Unfortunately, input power could not be measured with any degree of accuracy, consequently efficiency calculations could not be made to determine if fluid properties have any noticeable effect on this parameter. The table on figure 5 lists the significant differences in geometry, speed, and method of obtaining discharge pressures for the inducers used in the comparison.

Cavitating Performance

The general method of conducting cavitation tests is to maintain the flow geometry, hence flow coefficient, and observe the change in head rise as a function of some cavitation parameter. In order to minimize the testing time, the tests reported herein were conducted at constant-discharge throttle setting; consequently, constant flow coefficient performance had to be obtained by cross-plotting the data. Figure 6 presents the variation of head coefficient ψ with cavitation number k for constant values of flow coefficient φ.

A common feature of all these curves is that the head is essentially unaffected until a cavitation number of approximately 0.075 or less is reached, and then it drops off slowly down to k values of zero. Thus, it appears that, for this inducer, cavitation breakdown (where a further decrease of cavitation number results in a rapid deterioration of head rise) did not occur even down to computed k values of zero.

From the results of figure 6 the overall performance obtained under cavitating conditions as presented on figure 4 can be better identified. This is accomplished by fairing in constant k operating conditions as shown by the dashed lines (fig. 4). The dotted line outlines the data points at which Venturi instrumentation indicates that cavitation is probably occurring in the Venturi throat.

In the general area of a flow coefficient of 0.064 (same region as the dip appeared in the noncavitating performance characteristic) there is a general convergence of lines of constant k values. At a given flow coefficient in this area, the performance drop reaches a minimum as k is lowered from the noncavitating value of 0.075 to k = 0 (essentially a boiling fluid entering the pump). For this reason this area would be of interest as a design-point region.

As noted, the curves of figure 6 terminate at k = 0, a flow condition, by definition, in which the stream static pressure just equals the fluid vapor pressure. It is also evident from figure 4 that a large part of the pump performance recorded fell outside the flow regime bounded by the $k \geq 0.075$ (noncavitating) to k = 0 curves. At this point some consideration must be given to the type of flow anticipated in this area, the ability of the flow parameter (k, H_{SV}, etc.) to describe the flow condition, and the effect of the instrument location on these parameters.

As the decreasing supply tank pressure tends to force the inlet stream static pressure below the fluid vapor pressure, several basic inlet flow models are suggested:

(1) The fluid is carried along in a superheated state. In this case the stream static pressure would exist at a value lower than the fluid vapor pressure, with increasingly negative k values calculated as the supply tank pressure is lowered.

(2) Fluid is evaporated in the inlet sections leading to this pump. However, the heat absorbed in the evaporation of a portion of the flow sufficiently cools the remaining liquid to inhibit further vaporization. If this latter process is assumed to continue to a new equilibrium state, the stream static pressure approaches and finally again equals the local fluid vapor pressure. As the supply tank pressure is systematically reduced, at each new equilibrium state the computed k value, by definition, remains zero; but increasing amounts of vapor are formed in the inlet flow. Under these conditions the k parameter alone no longer would completely describe the inlet flow conditions as experienced by the pump.

For an installation with the pump mounted in a line with a decreasing total-pressure level along the flow path, the formation of vapor would be expected to occur at increasingly greater distances from the pump inlet as the supply tank pressure is reduced. Consequently, inlet flow conditions can be adequately recorded only if the instrumentation is located at the inlet face of the inducer. This points up the necessity of carefully locating instrumentation if inlet flow conditions for k = 0 mode of operations are to be accurately measured.

The data points of figure 4 indicate the decreasing level of performance at a constant throttle setting as the supply tank pressure is lowered from the value necessary for initial $k = 0$ operation. In this same flow regime, table I further indicates that, with the exception of one series of operating conditions (runs 46 to 59), the inlet temperature drops off rapidly with decreasing inlet pressure. This implies that some evaporative cooling was taking place, and the second flow model applies. However, since the latent heat of evaporation is obtained from the liquid surrounding the vapor bubbles and as such is a time-dependent process, it is probable that both flow models are present to some extent. With the present instrumentation it was impossible to determine any individual effects. Because of the time-dependent nature of the process, another pump with different inlet conditions ($V_{a,1}$, e.g.) might be expected to have a different ratio of superheat and evaporative cooling for the same type of operation.

The negative k values shown in table I are based on static pressure at the inducer inlet (as computed from the measured liquid flow only and the inlet area) and a vapor pressure computed from carbon resistor temperature measured several inches upstream of the inducer inlet. For these reasons little significance is placed on the values calculated, although it is interesting to note that they remain essentially constant as inlet pressure is reduced below the $k = 0$ flow condition.

It should be noted here that operation at inlet pressures of atmospheric or below was attained by initating operation at a high suction pressure and then systematically reducing the supply tank pressure. It is possible that if the initial pump operation were attempted at these low inlet pressures the pump would not start, that is, would not pump a liquid.

Figure 7 compares the cavitation performance of the 83° helical inducer tested in liquid hydrogen with the cavitation performance of similar types of inducers operated in water. For each inducer, an attempt was made to select a constant flow coefficient performance curve maintaining good performance to low k values. Figure 7 demonstrates the ability of pumps to operate in liquid hydrogen at lower k values (or H_{SV}) for a given drop in performance and concurs with the results of earlier works. Thus far, however, attempts at correlating the cavitation results in water with those obtained in other fluids have had limited success, especially in the field of cryogenic liquids (see refs. 2 and 3).

In order to relate the data expressed in terms of cavitation number k to the familiar suction specific speed parameter, approximate relations are noted in the table on figure 7. The data presented herein provide additional encouragement that high suction specific speeds may be expected when operating in liquid hydrogen.

[redacted]

The radial variations of pump head rise at three values of flow coefficient are presented in figure 8 both for the noncavitating and $k = 0$ mode of performance. The radial gradient of head coefficient observed for the noncavitating condition is characteristic of the helical surface blade. As the flow coefficient is reduced (increased incidence), the gradient of head coefficient increases, the head rise in the tip region increasing much faster than in the hub region. An analytical study of the effects of geometry and losses on the performance parameters of flat-plate helical inducers is presented in reference 8.

A notable feature of the radial distributions observed at $k = 0$ operation was that the latter followed noncavitating performance very closely. At the low and high flow coefficients the decrease in head rise is nearly the same at all radii as the mode of operation is varied from a noncavitating to a cavitating condition. At the mean flow a slight redistribution of head rise appears to occur. This was noted for several data points taken in this region of flow.

CONCLUDING REMARKS

The investigation reported herein presents the data obtained from a specific helicoidal inducer. As much as possible, the data have been presented in a form which eliminates any effects of this particular inducer or test set-up. The exception to the latter is the form of the constant-throttle curve (data points of fig. 4), which does show system effects.

The noncavitating performance showed an overall head characteristic curve similar to those obtained from inducers operating in water. Little change would be expected if this inducer were operated in a different fluid. The measured radial gradient of noncavitating head coefficient (increasing with radius) follows the energy input gradient inherent in the flat-plate helical inducer. The gradient increased as the flow coefficient was decreased.

The cavitation data indicate that the inducer performance dropoff in liquid hydrogen is relatively small as the mode of operation is changed from $k > 0.075$ (noncavitating) to $k = 0$ (boiling fluid at inducer inlet) for a constant value of flow coefficient. The surveys of discharge total pressure from radial rakes further indicated that this dropoff occurred at all radii and in approximately equal amounts except for a mean flow coefficient where the decrease occurs from the mean to the tip region performances.

Comparison of the results of this inducer with similar inducers operated in water confirmed the findings of other investigations that, for a given drop in performance, inducers will operate in liquid hydrogen to significantly lower values of cavitation number, or net positive

suction head. Conversely, inducers employed in liquid hydrogen may be expected to attain larger values of suction specific speed.

A very interesting feature is the observed range of performance over which the inducer pumped essentially a boiling fluid. Several inlet flow models are proposed to aid in an understanding of the inlet conditions as experienced by the pump. While the data supply evidence that the flow model employing evaporative cooling occurred (and probably predominated) in this case, the instrumentation was not sufficient, or sensitive enough, to preclude the possibility of some superheat (other flow model) in the fluid. Speculation that the time-dependency aspects of the process would diversely affect the inlet flow conditions of each different inducer is made. The need for better measuring devices and for careful location of the measuring stations, particularly when in the above flow regime, is noted.

Lewis Research Center
National Aeronautics and Space Administration
Cleveland, Ohio, November 16, 1960

[redacted]

APPENDIX - OPERATIONAL AND MECHANICAL EXPERIENCES

Because of the unique properties of liquid hydrogen it appeared that certain rig details and operating procedures not pertinent to the theme of the main text would be of interest to the reader. Therefore, a discussion of these items will be presented in the following paragraphs.

A carbon seal with a mechanical carbon nosepiece having impregnation of metal fluoride was used in both the face and shaft seals near the inducer rotor. The metal fluoride serves as an additive to assist in the formation of a lubricating film of graphite on the mating surfaces. Because of previous seal failures with carbon and aluminum, a 304 stainless-steel ring was fitted and shrunk on the rear face of the inducer impeller to act as the rubbing surface. The face seal pressure used was 20 pounds per square inch gage. No functional starting difficulties were incurred with this seal pressure.

Each of the two pump shaft bearings (standard clearance), which were designed to be oil-lubricated, was provided with electric heating coils to help maintain reasonable working temperatures.

Before liquid or gaseous hydrogen was introduced into the test system, the system was thoroughly purged. The purge method consisted of (1) evacuating system to 15 inches of mercury (2) pressurizing system to 10 pounds per square inch with helium gas (3) opening momentarily each of the vent valves in the system. Complete purging was assured by repeating this procedure (two or three times).

In order to ensure reliable vapor pressure for the H_{SV} meter, the vapor bulb was pressurized with hydrogen gas directly from the supply Dewar. Before the vapor bulb was filled, the supply Dewar was vented to atmospheric pressure and, by use of integral heat-exchanger coils, self-pressurized to 40 pounds per square inch gage. The actual procedure used to prepare the vapor bulb for test operation was as follows:

(1) evacuate bulb to a minimum of 28 inches mercury

(2) pressurize bulb with 40 pounds per square inch gage hydrogen gas

(3) repeat above steps six times

In order to help maintain reasonable bearing temperatures, the inducer was operated at a base speed of about 9000 rpm, while the system was chilled and filled with liquid hydrogen. During this time, oil lubrication to the pump bearings was stopped, although scavenge pressure was still maintained. Only occasional lubrication during ensuing test runs was used with the pump bearings.

REFERENCES

1. Ross, C. C., and Banerian, Gordon: Some Aspects of High-Suction Specific-Speed Pump Inducers. Trans. ASME, vol. 78, no. 8, Nov. 1956, pp. 1715-1721.

2. Jacobs, Robert B., Martin, Kenneth B., Van Wylen, Gordon J., and Birmingham, Bascom W.: Pumping Cryogenic Liquids. Tech. Memo. 36, Rep. 3569, Cryogenic Eng. Lab., NBS, Feb. 24, 1956.

3. Stahl, H. A., and Stepanoff, A. J.: Thermodynamic Aspects of Cavitation in Centrifugal Pumps. Trans. ASME, vol. 78, no. 8, Nov. 1956, pp. 1691-1693.

4. Lewis, George W., Tysl, Edward R., and Hartmann, Melvin J.: Design and Experimental Performance of a Small Centrifugal Pump for Liquid Hydrogen. NASA TM X-388, 1960.

5. Jacobs, Robert B., Martin, Kenneth B., and Hardy, Richard J.: Direct Measurement of Net Positive Suction Head. Rep. 5500, NBS, July 18, 1957.

6. Crouse, James, Montgomery, John C., and Soltis, Richard F.: Investigation of the Performance of an Axial-Flow-Pump Stage Designed by the Blade-Element Theory - Design and Overall Performance. NASA TN D-591, 1960

7. Acosta, A. J.: An Experimental Study of Cavitating Inducers. Second Symposium of Naval Hydrodynamics, Office Naval Res., Aug. 1958.

8. Montgomery, John C.: Analytical Performance Characteristics and Outlet Flow Conditions of Constant and Variable Lead Helical Inducers for Cryogenic Pumps. NASA TN D-583, 1960.

TABLE I. - EXPERIMENTAL DATA COMPARISONS

[Approx. $Q_{gpm} = 2110\,\varphi$; conversion, $H_{ft} = 2610\,\psi$.]

Run number	Head coeff., ψ, dimensionless	Flow coeff., φ, dimensionless	H_{sv} transducer range, lb/sq in.	Inlet total pressure, lb/sq in. abs	T_l, based on carbon resistors, °R	T, based on vapor bulb, °R	k, based on vapor bulb	k, based on carbon resistors
12	0.2541	0.0347	40	23.69	37.8	37.21	0.179	0.145
13	.2529	.0386	40	22.85	37.8	37.07	.169	.126
14	.2549	.0347	40	21.97	37.8	37.13	.143	.103
15	.2530	.0357	40	19.01	37.8	37.10	.070	.027
16	.2511	.0354	2.0	17.69	37.6	37.15	.033	.007
17	.2504	.0357	2.0	17.73	37.6	37.14	.034	.008
18	.2433	.0347	2.0	16.77	37.4	37.04	.017	-.003
19	.2453	.0348	2.0	16.81	37.4	37.14	.011	-.002
20	.2396	.0348	2.0	16.05	37.2	37.18	-.010	-.009
21	.2408	.0348	2.0	16.29	37.2	37.15	-.003	-.003
22	.2534	.0352	2.0	17.77	37.7	37.14	.035	.018
23	.2534	.0360	2.0	18.27	37.7	37.21	.046	.017
24	.2433	.0350	2.0	16.93	37.4	37.14	.014	.001
25	.2400	.0349	2.0	16.37	37.3	37.05	.006	-.008
26	.2385	.0347	2.0	16.13	37.2	37.06	-.001	-.007
27	.2354	.0340	2.0	15.89	37.1	37.05	-.006	-.007
28	.2408	.0347	2.0	16.17	37.3	37.10	-.003	-.013
29	.1771	.0313	----	14.25	36.3	36.32	-.001	-.003
30	.2519	.0307	40	35.73	38.5	37.98	.430	.397
34	.2632	.0307	40	20.61	38.3	37.60	.078	.030
35	.2585	.0306	40	19.53	38.3	37.58	.051	.003
36	.2585	.0294	2.0	19.33	38.2	37.67	.041	.006
37	.2522	.0307	2.0	18.65	38.1	37.64	.025	-.005
38	.2405	.0287	2.0	17.57	37.8	37.49	.008	-.009
39	.2484	.0290	2.0	17.61	37.8	37.51	.008	-.008
40	.2468	.0293	2.0	17.89	37.9	37.58	.010	-.008
41	.2368	.0296	----	17.01	37.6	37.37	-.003	-.010
42	.2265	.0268	----	16.37	37.4	37.16	-.001	-.013
43	.2176	.0279	----	16.29	37.3	37.13	-.001	-.009
44	.2064	.0274	----	16.13	37.1	37.07	-.001	0
46	.1797	.0618	40	27.73	38.1	37.94	.229	.222
47	.1884	.0601	40	23.41	37.8	37.63	.144	.137
49	.1931	.0587	40	20.45	37.9	37.70	.065	.054
50	.1917	.0596	2.0	19.37	37.8	37.75	.034	.034
51	.1947	.0579	2.0	18.97	37.8	37.81	.020	.024
52	.1904	.0563	2.0	18.69	37.8	37.79	.014	.017
53	.1917	.0586	2.0	18.69	37.8	37.91	.005	.017
54	.1903	.0573	2.0	18.37	37.8	37.85	.002	.009
55	.1892	.0558	2.0	18.69	37.9	38.01	-.003	.009
56	.1893	.0558	2.0	18.73	38.0	38.09	-.008	.004
57	.1750	.0537	2.0	19.41	38.2	38.22	.001	.005
58	.1502	.0514	2.0	19.41	38.1	38.31	.006	.013
59	.1410	.0479	2.0	18.69	38.0	38.02	.002	.004
60	.2061	.0536	40	32.21	38.1	37.78	.358	.339
61	.2199	.0521	40	28.25	38.0	37.73	.260	.246
62	.2193	.0482	40	24.53	38.0	37.78	.165	.153
63	.2238	.0503	40	21.57	38.0	37.50	.108	.077
64	.2223	.0480	40	19.85	37.9	37.58	.059	.040
65	.2261	.0463	2.0	18.97	37.8	37.56	.038	.025
66	.2203	.0470	2.0	18.21	37.8	37.63	.013	.006
67	.2197	.0467	2.0	17.61	37.6	37.52	.006	.004
68	.2196	.0445	----	17.49	37.6	37.41	.010	.001
69	.2147	.0435	2.0	17.05	37.5	37.52	.008	-.004
70	.1930	.0428	----	15.97	37.1	37.01	-.002	-.005
71	.1882	.0422	----	15.89	37.0	36.98	-.002	0
72	.1815	.0407	----	15.53	36.9	36.84	-.002	-.003
73	.1702	.0399	----	15.17	36.8	36.70	-.002	-.005
74	.1300	.0395	----	14.45	36.4	36.40	-.002	-.001
75	.1501	.0395	----	14.37	36.5	36.36	-.002	-.007
76	0.1300	0.0738	40	32.49	37.9	37.82	0.358	0.355
77	.1511	.0721	40	27.65	37.8	37.75	.240	.240
78	.1639	.0674	40	23.37	37.8	37.73	.136	.135
79	.1759	.0649	40	19.53	37.8	37.58	.047	.037
80	.1746	.0642	2.0	19.29	37.8	37.65	.038	.031
81	.1760	.0641	2.0	18.69	37.7	37.59	.026	.022
82	.1733	.0640	2.0	17.97	37.7	37.55	.011	.004
83	.1759	.0628	2.0	17.73	37.6	37.61	.001	.005
84	.1770	.0614	----	17.33	37.5	37.54	-.004	.001
85	.1666	.0614	----	17.01	37.4	37.41	-.004	0
86	.1502	.0580	----	16.29	37.3	37.13	-.004	-.012
87	.1388	.0559	----	15.89	37.0	36.98	-.003	-.001
88	.0637	.0915	40	24.89	37.9	38.00	.149	.160
89	.0624	.8999	40	24.69	37.8	37.90	.151	.162
90	.0724	.0900	40	22.69	37.8	37.78	.112	.114
91	.0842	.0860	40	21.41	37.8	37.89	.072	.082
92	.0964	.0815	40	19.69	37.8	37.86	.031	.039
93	.0933	.0784	2.0	19.29	37.8	37.82	.024	.028
94	.0984	.0786	2.0	18.65	37.7	37.79	.011	.019
95	.0994	.0782	2.0	18.21	37.6	37.84	-.005	.015
96	.0962	.0760	2.0	17.81	37.6	37.76	-.008	.006
97	.0924	.0719	----	17.21	37.4	37.49	-.005	.004
98	.0872	.0683	----	16.85	37.4	37.35	-.005	-.005
99	.0823	.0652	----	16.41	37.2	37.18	-.004	-.003
100	.0733	.0623	----	16.09	37.1	37.05	-.004	-.004
101	.0913	.0822	40	26.74	37.8	37.69	.217	.214
102	.1067	.0800	40	23.26	37.7	37.68	.134	.135
103	.1191	.0771	40	20.58	37.6	37.74	.062	.075
104	.1258	.0737	2.0	18.30	37.7	37.58	.016	.011
105	.1275	.0714	2.0	17.82	37.6	37.63	.001	.006
106	.1247	.0716	2.0	17.58	37.6	37.63	-.005	0
107	.1070	.0661	----	16.38	37.3	37.16	-.005	-.011
108	.0998	.0615	----	15.98	37.0	37.01	-.004	0
109	.0905	.0611	----	15.90	37.0	36.98	-.004	-.002
115	.0372	.0494	----	13.57	36.0			.005
116	.0359	.0519	----	14.77	36.3			.014
117	.0362	.0599	----	15.84	36.5			.028
118	.0350	.0640	2.0	16.25	36.7			.025
119	.0369	.0680	2.0	16.73	36.8			.032
120	.0377	.0744	2.0	17.82	37.1			.037
121	.0379	.0774	40	19.37	37.4			.057
122	.0417	.0848	40	20.23	37.7			.058
123	.0442	.0871	40	20.63	37.9			.054
124	.0426	.0890	40	21.25	38.0			.062
125	.0396	.0944	40	21.37	38.0			.065
126	.0354	.0954	40	21.03	37.9			.062
127	.0319	.0984	40	21.22	37.8			.074
128	.0315	.0982	40	21.39	37.9			.071
129	.0326	.0982	40	21.27	37.9			.068
130	.0318	.0986	40	21.27	37.9			.068
131	.0315	.0985	40	20.87	37.9			.065

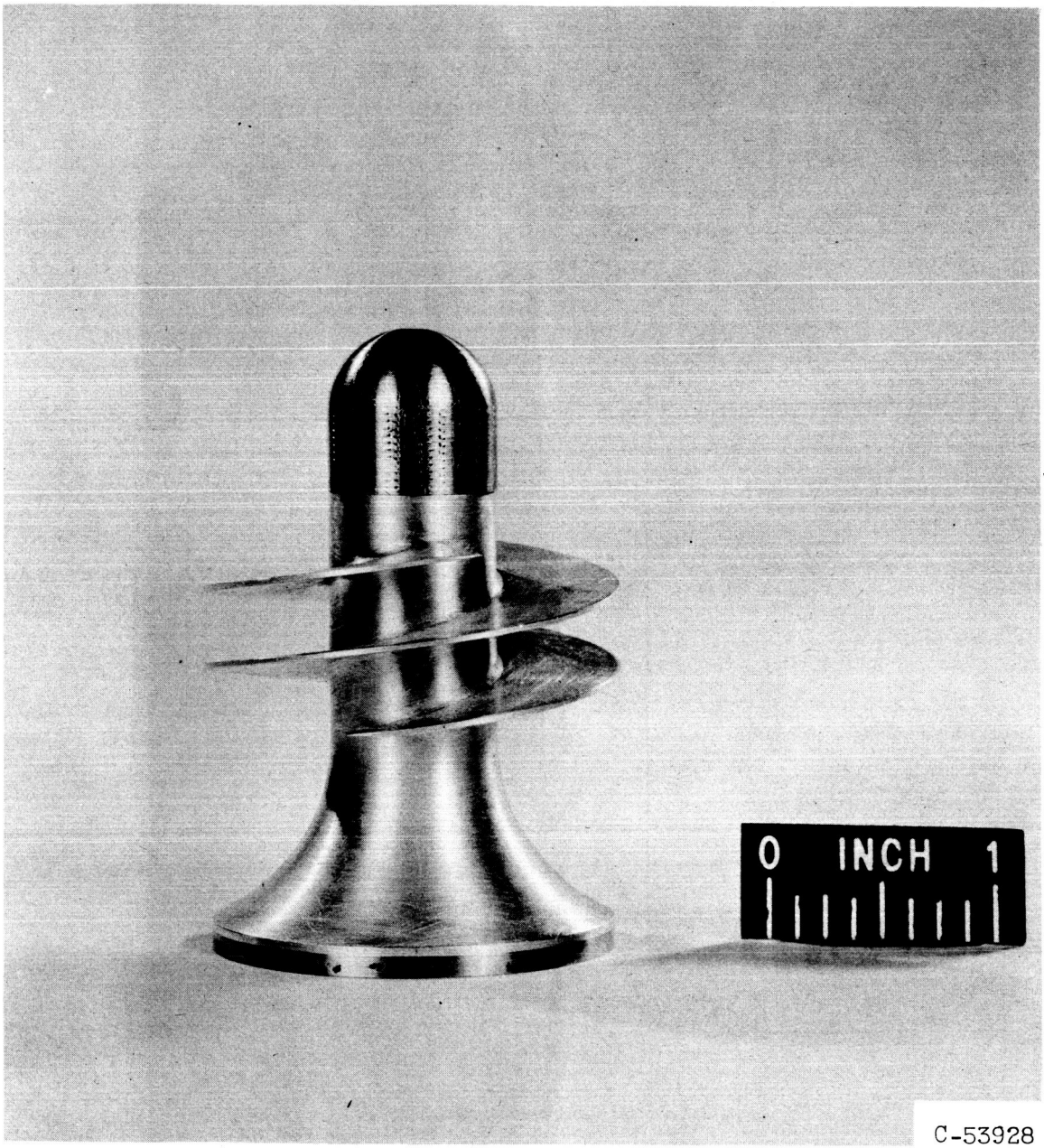

Figure 1. - 83° Flat-plate helical inducer.

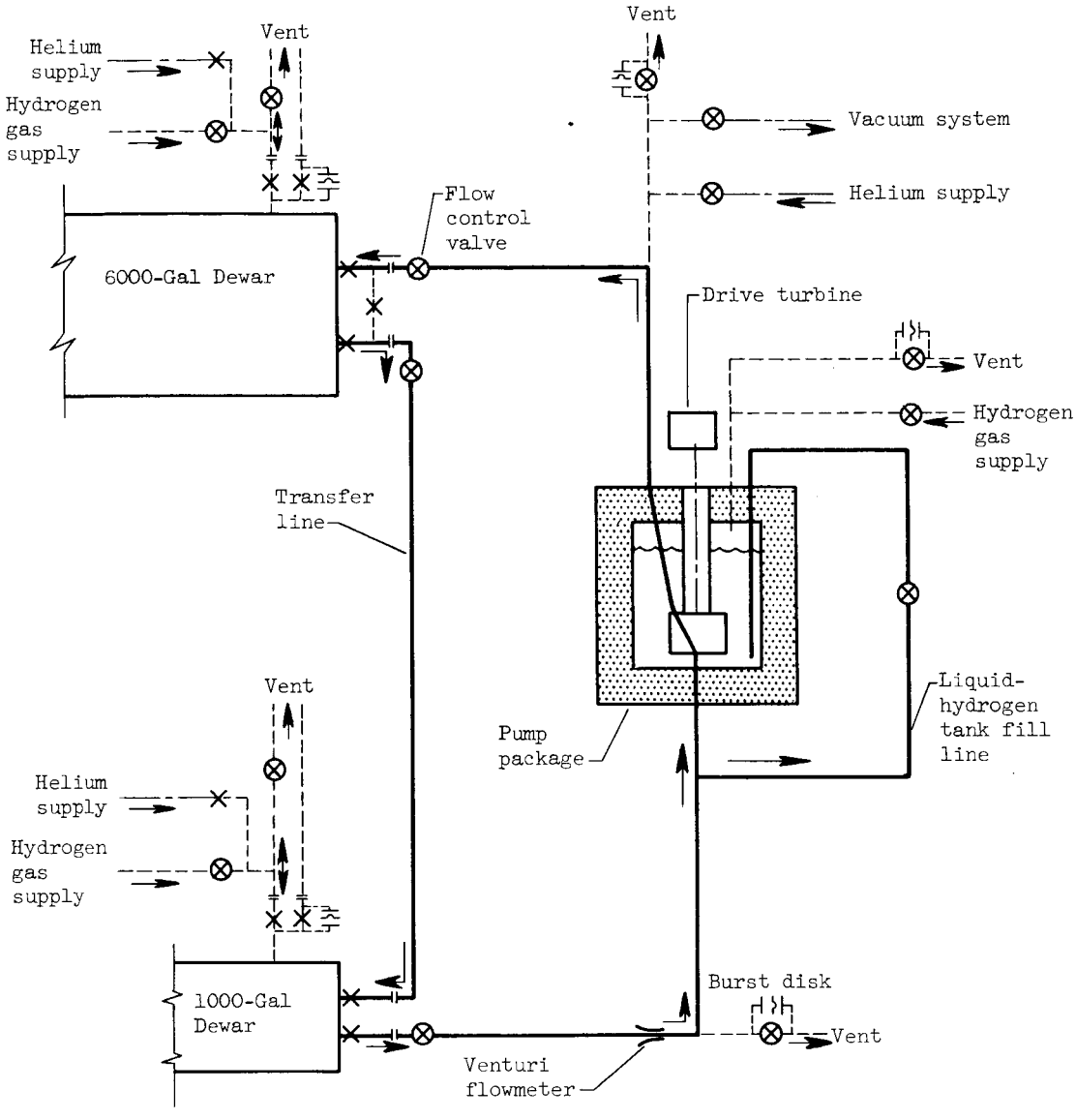

Figure 2. - Schematic diagram of inducer test facility.

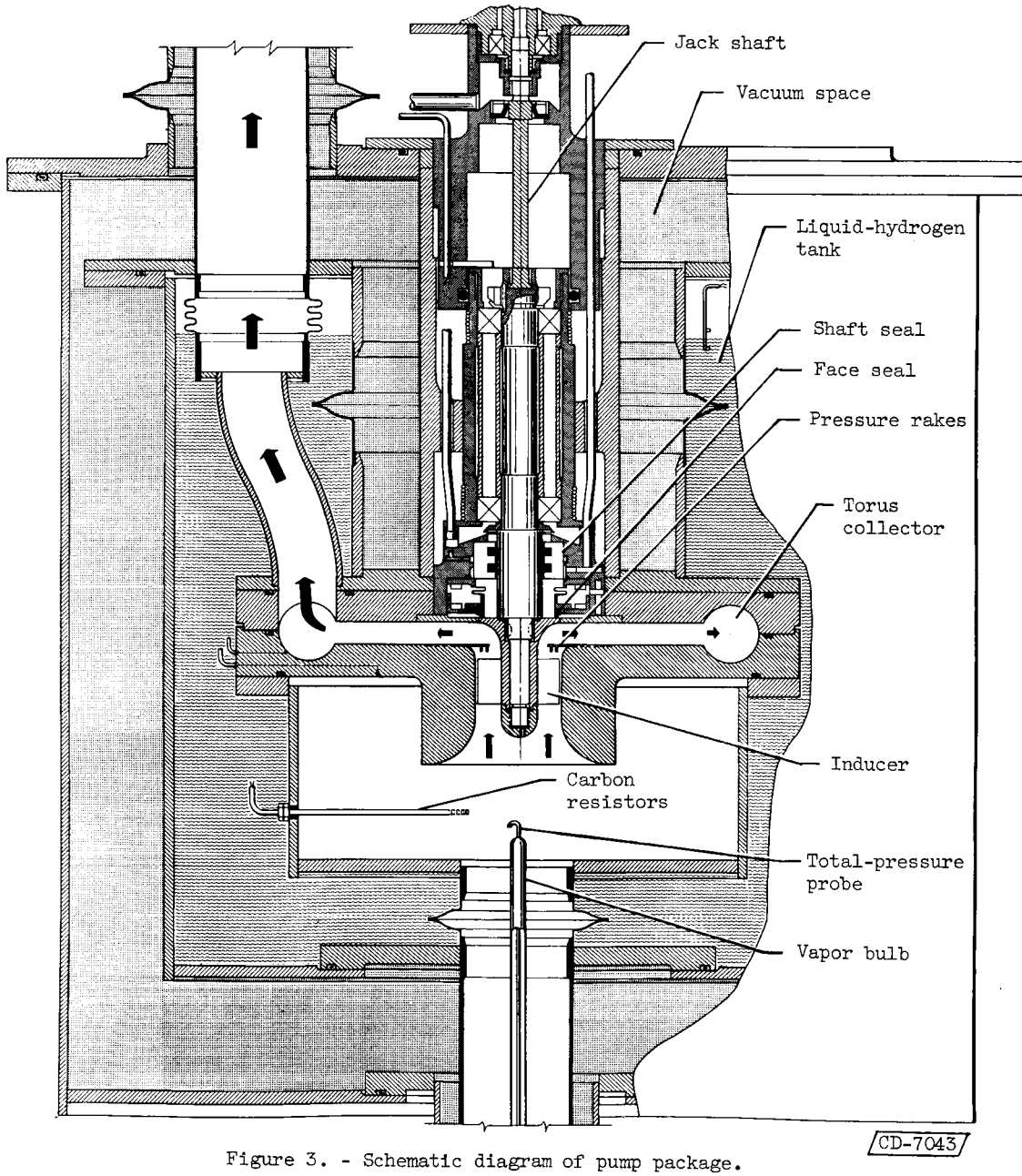

Figure 3. - Schematic diagram of pump package.

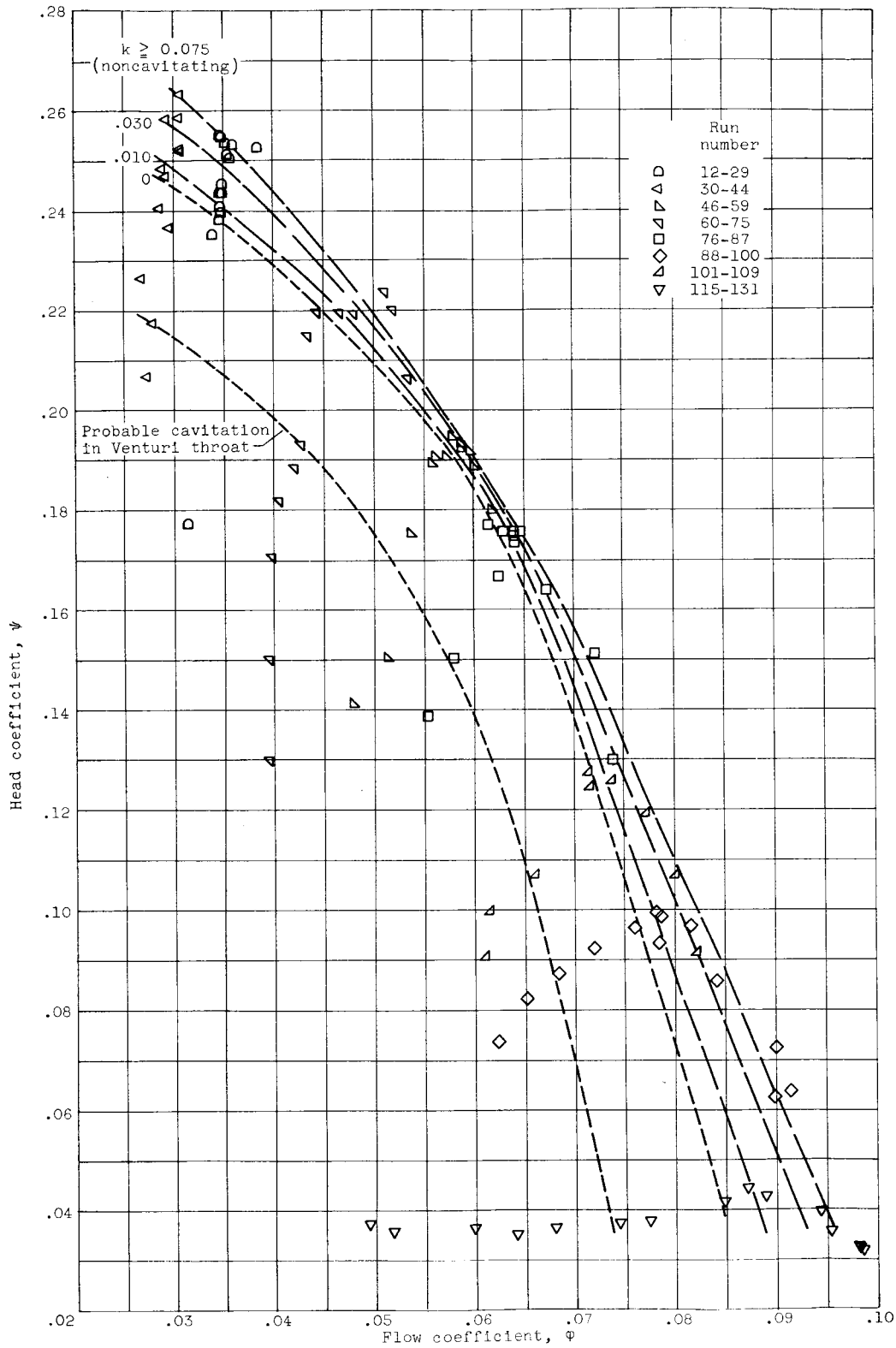

Figure 4. - Overall performance of 83° helical inducer in liquid hydrogen.

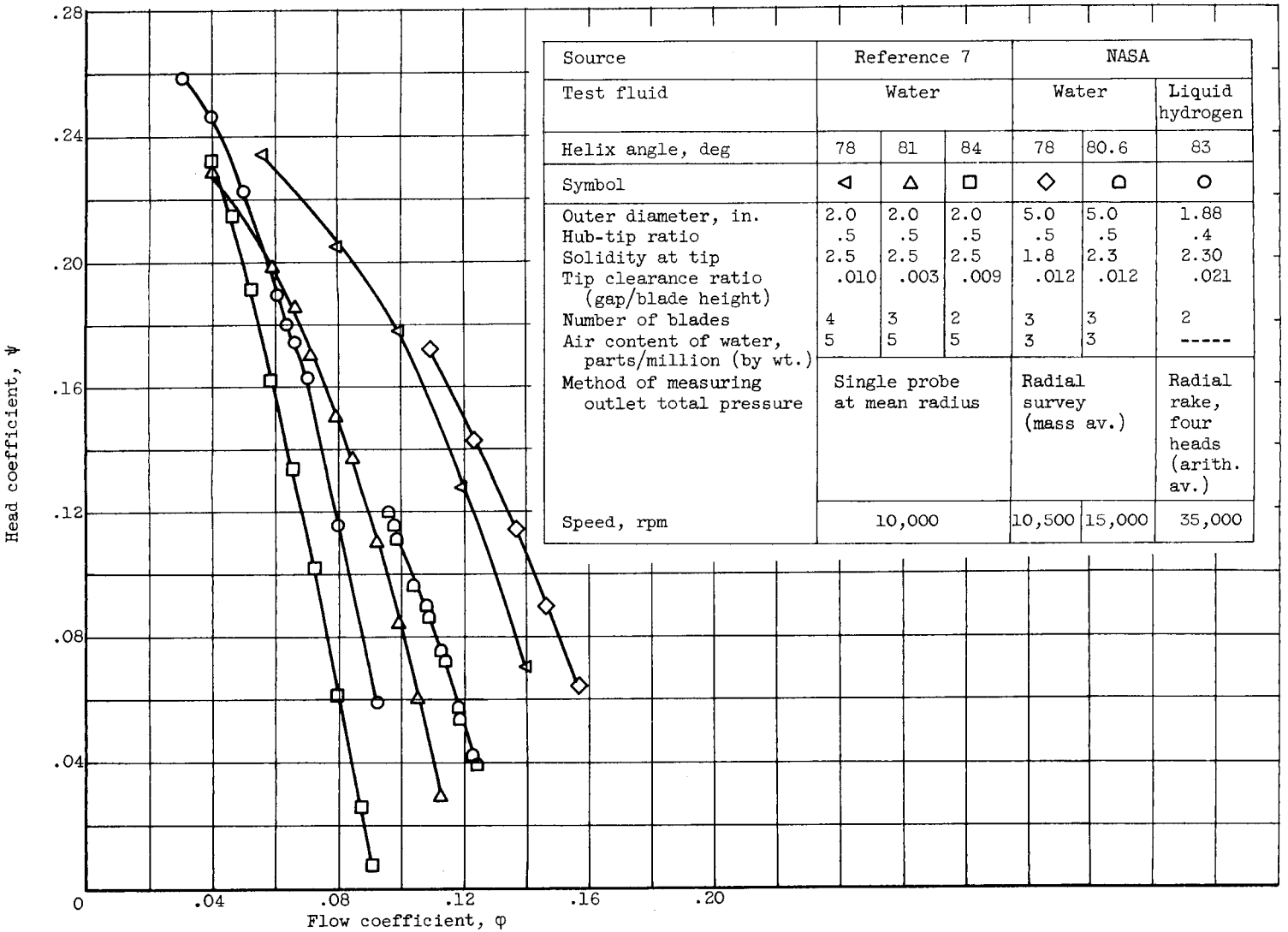

Source	Reference 7			NASA		
Test fluid	Water			Water		Liquid hydrogen
Helix angle, deg	78	81	84	78	80.6	83
Symbol	◁	△	□	◇	⌂	○
Outer diameter, in.	2.0	2.0	2.0	5.0	5.0	1.88
Hub-tip ratio	.5	.5	.5	.5	.5	.4
Solidity at tip	2.5	2.5	2.5	1.8	2.3	2.30
Tip clearance ratio (gap/blade height)	.010	.003	.009	.012	.012	.021
Number of blades	4	3	2	3	3	2
Air content of water, parts/million (by wt.)	5	5	5	3	3	-----
Method of measuring outlet total pressure	Single probe at mean radius			Radial survey (mass av.)		Radial rake, four heads (arith. av.)
Speed, rpm	10,000			10,500	15,000	35,000

Figure 5. - Noncavitating performance comparison of several helical inducers.

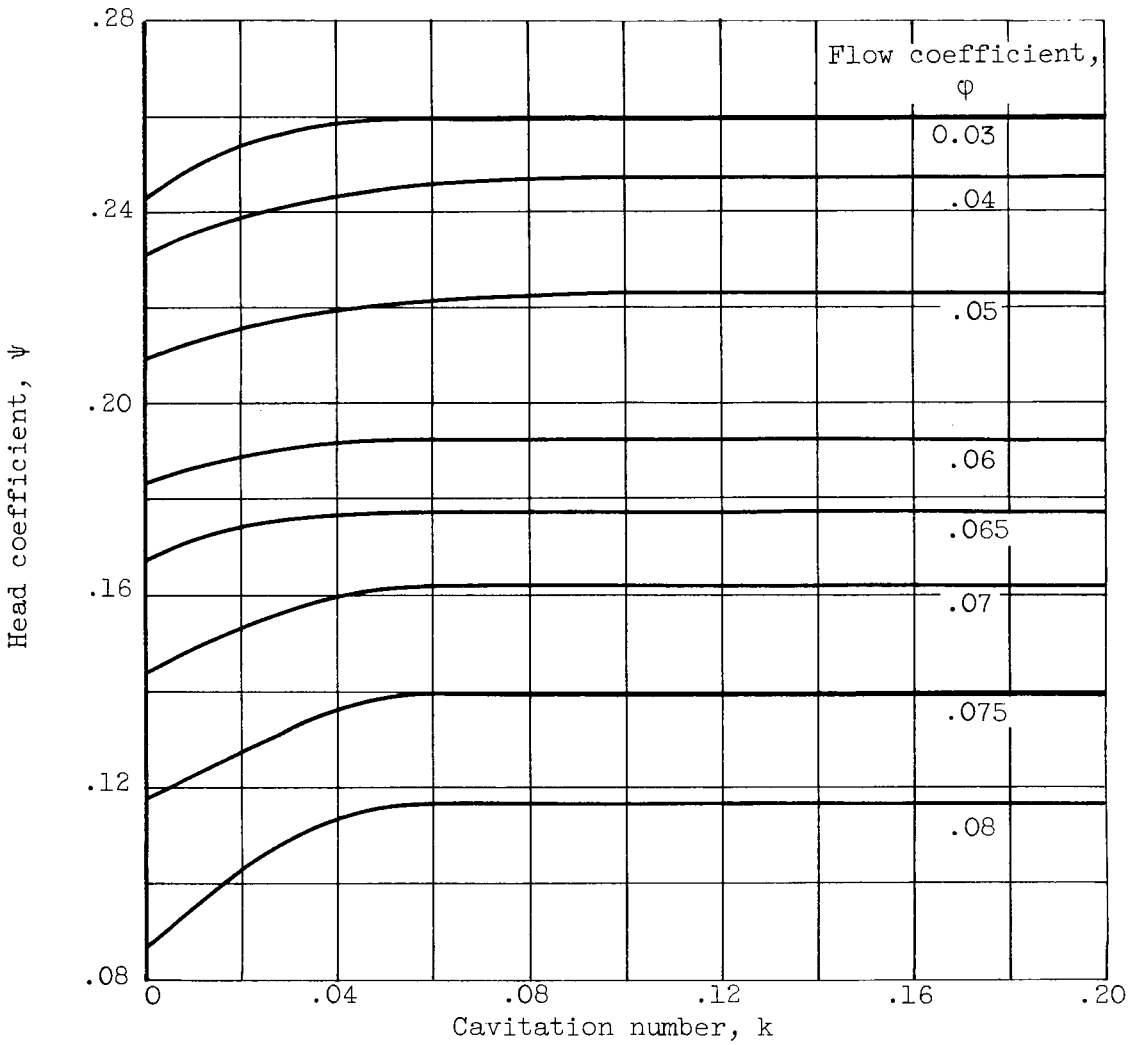

Figure 6. - Cavitation performance of 83° helical inducer in liquid hydrogen.

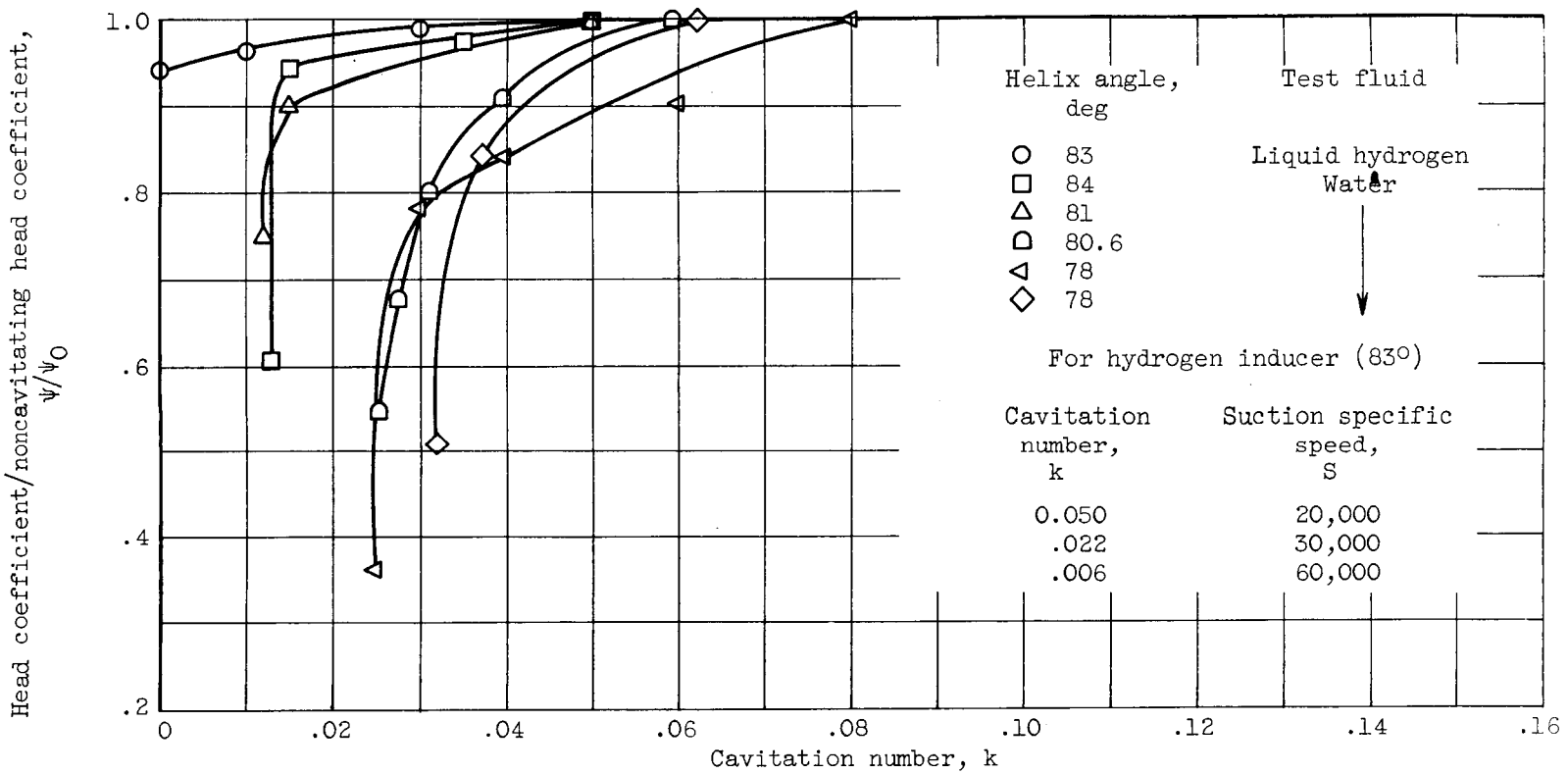

Figure 7. - Cavitation performance comparison of helical inducers in water and liquid hydrogen.

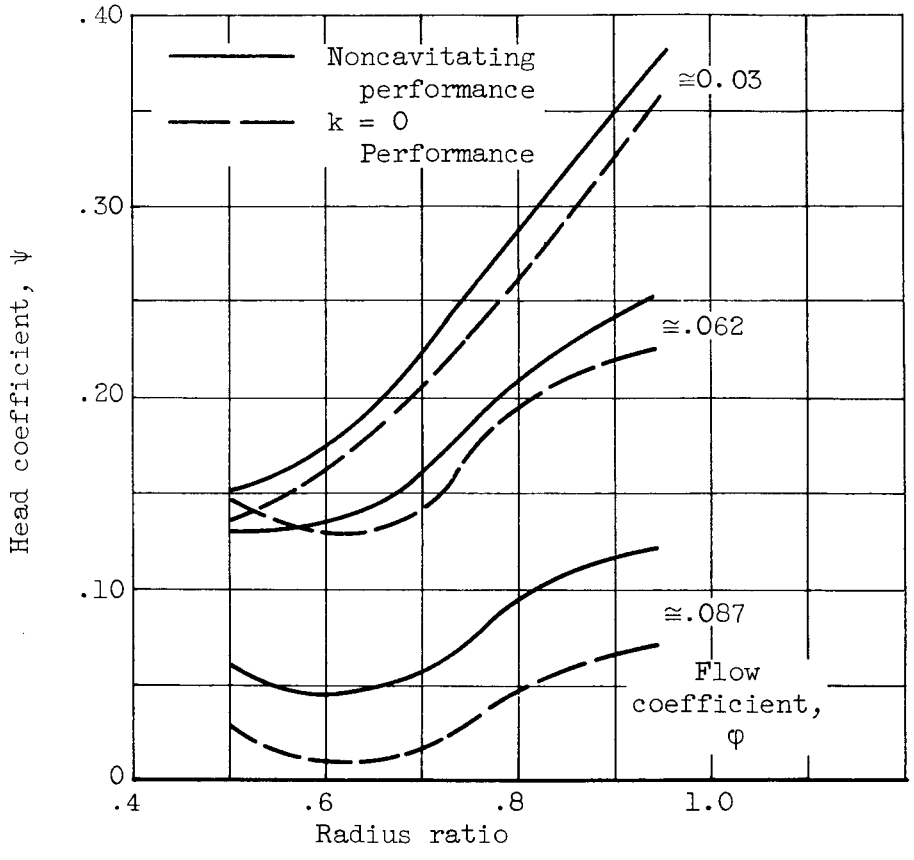

Figure 8. - Head coefficient plotted against radius ratio at several flow coefficient values for 83° helical inducer tested in liquid hydrogen.